Journal of Power Sources 273 (2015) 298–304

Contents lists available at ScienceDirect

Journal of Power Sources

journal homepage: www.elsevier.com/locate/jpowsour

A dinuclear copper(II) electrocatalyst both water reduction and oxidation

Ling-Ling Zhou, Ting Fang, Jie-Ping Cao, Zhi-Hong Zhu, Xiao-Ting Su, Shu-Zhong Zhan*

College of Chemistry and Chemical Engineering, South China University of Technology, Guangzhou 510640, China

HIGHLIGHTS

- $Cu(Me_2oxpn)Cu(OH)_2$] **1** can catalyze both water oxidation and reduction to provide O_2 and H_2, respectively.
- **1** can catalyze water reduction to generate H_2, with a TOF of 654 (pH 7.0) moles h^{-1} at an overpotential of 789 mV *vs* SHE.
- **1** can also catalyze water oxidation at an overpotential of 636 mV *vs* SHE to give O_2 with a TOF of ~2.14 s^{-1} (pH 10.4).
- Sustained water reduction catalysis to give H_2 over a 32 h electrolysis period with 95% Faradaic yield.

GRAPHICAL ABSTRACT

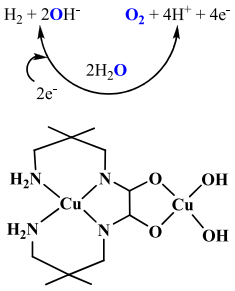

ARTICLE INFO

Article history:
Received 18 July 2014
Received in revised form
27 August 2014
Accepted 10 September 2014
Available online 18 September 2014

Keywords:
Water soluble copper(II) electrocatalyst
Water reduction
Water oxidation
Hydrogen evolution

ABSTRACT

Splitting water is a key challenge in the production of chemical fuels from electricity. Although several catalysts have been developed for these reactions, substantial challenges remain towards the ultimate goal of an efficient, inexpensive and robust electrocatalyst. Until now, there is as yet no report on both water oxidation and reduction by identical catalyst. Reported here is the first soluble copper-based catalyst, $Cu(Me_2oxpn)Cu(OH)_2$] **1** (Me_2oxpn: N,N′-bis(2,2′-dimethyl-3-aminopropyl)oxamido) for both electrolytic water oxidation and reduction. Water oxidation occurs at an overpotential of 636 mV *vs* SHE to give O_2 with a turnover frequency (TOF) of ~2.14 s^{-1}. Electrochemical studies also indicate that **1** is a soluble molecular species, that is among the most rapid homogeneous water reduction catalysts, with a TOF of 654 mol of hydrogen per mole of catalyst per hour at an overpotential of 789 mV *vs* SHE (pH 7.0). Sustained water reduction catalysis occurs at glassy carbon (GC) to give H_2 over a 32 h electrolysis period with 95% Faradaic yield and no observable decomposition of the catalyst.

1. Introduction

Splitting water into hydrogen and oxygen is one of the most attractive scenarios for solar energy harvesting and sustainable energy production [1–5]. This endergonic electrochemical conversion stores 1.23 V and consists of the four electrons, four proton oxidation of water to oxygen and the reduction of the produced protons to hydrogen. One of the key challenges to water splitting is the development of efficient catalysts. These considerations have led to the development of molecular catalysts employing the more transition abundant metals, and several complexes based on nickel [6–11], cobalt [12–16] and molybdenum [17,18] have been developed as electrocatalysts for the reduction of water to form H_2. However, the search for robust and

* Corresponding author. Fax: +86 20 87112053.
E-mail address: shzhzhan@scut.edu.cn (S.-Z. Zhan).

http://dx.doi.org/10.1016/j.jpowsour.2014.09.075
0378-7753/

highly active catalysts for hydrogen evolution that can operate in purely aqueous solution by electrochemical approaches still remains a great challenge. Another notable progress has been made in homogeneous water oxidation catalysis with transition metal complexes, including manganese [18–20], cobalt [21–23], copper [24,25] and iron [26–31]. Despite much progress in water oxidation and reduction catalysis, major improvements in several areas, including lowering overpotentials, increasing catalyst durability, and using earth abundant elements, are needed before efficient electrocatalytic water splitting can be realized. In designing a model featuring both water oxidation and reduction functionality, we sought a synthetic cofactor with the following inspired properties: (1) The metal center coordination geometry is planar; (2) Mild redox couple closer to the H_2/H^+ couple and O_2/H_2O couple, in the range −0.75 to −1.45 V and 0.40–1.23 V versus SHE, respectively; (3) Chemical inertness, so that reactions would be localized at the metal centers. Until now, there is as yet no report on both water oxidation and reduction by identical catalyst. Reported here is a water soluble dinuclear copper electrocatalyst, [Cu(Me_2oxpn)Cu$(OH)_2$] **1** that can catalyze both water oxidation and reduction.

2. Experimental

2.1. Materials and physical measurements

All commercially available reagents were used as received without further purification. Cyclic voltammograms were obtained on a CHI-660E electrochemical analyzer under oxygen-free conditions using a three-electrode cell in which a glassy carbon electrode was the working electrode, a saturated Ag/AgCl electrode was the reference electrode, and platinum wire was the auxiliary electrode. Controlled-potential electrolysis (CPE) in aqueous media was conducted using an air-tight glass double-compartment cell separated by a glass frit. The working compartment was fitted with a glassy carbon plate or an ITO plate and an Ag/AgCl reference electrode. The auxiliary compartment was fitted with a Pt gauze electrode. The working compartment was filled with 50 mL of 0.25 M phosphate buffer solution at different pH values, while the auxiliary compartment was filled with 35 mL phosphate buffer solution. Complex **1** was then added and cyclic voltammograms were recorded. After electrolysis, a 0.5 mL aliquot of the headspace was removed and replaced with 0.5 mL of CH_4. A sample of the headspace was injected into the gas chromatograph (GC). GC experiments were carried out with an Agilent Technologies 7890A gas chromatography instrument. UV–vis spectra were recorded on a U-3900H spectrophotometer. ICP of a glassy carbon electrode after 2 h electrolysis was recorded on a PHILIPS XL-30ESEM spectrometer.

2.2. Syntheses of [Cu(Me_2oxpn)Cu$(OH)_2$] 1

1 was prepared by modification of the literature procedures [32,33]. To a solution of 0.04 mol of 2,2′-dimethyl-1,3-propylenediamine (4.08 g) in 15 mL of ethanol cooled by an ice bath was added dropwise a solution of 0.02 mol of diethyl oxalate (2.93 g) in 20 mL of ethanol. The mixture was heated at reflux for 2 h and then cooled down. A 0.044 mol sample of copper(II) hydroxide (prepared from the reaction of $CuSO_4 \cdot 5H_2O$ (10.99 g, 0.044 mol) with NaOH (3.52 g, 0.088 mol)) in suspension in 250 mL of water was added, which led to a deep blue solution. The mixture was filtered. The solid residue was washed with water in order to extract the expected compound. The solution was allowed to evaporate, affording deep blue small crystals, which were collected and dried in *vacuo* (6.84 g, 74.51% based on $CuSO_4 \cdot 5H_2O$). Calcd for $C_{12}H_{26}N_4Cu_2O_4$: C, 34.52; H, 6.23; N, 13.43. Found: C, 34.94; H, 6.32; N, 13.38. [H_2O, λ_{max}/nm (ε/L mol^{-1} cm^{-1})]: 234 (1.814×10^4), 599 (130).

3. Results and discussion

3.1. General characterization for complex 1

[Cu(Me_2oxpn)Cu$(OH)_2$] is very soluble in water and insoluble in organic solvents, such as methanol and ethanol. The UV–vis spectrum was recorded in aqueous solution, with main features at 234 nm (ε = 18,140) and 599 nm (ε = 130) (Fig. S1). The shoulder observed at 234 nm corresponds to a LMCT transition between the ligands and copper ions; The band observed at 599 nm is characteristic of Cu(II) d–d transitions. Similar UV–visible features have been observed for several similar dicopper(II) complexes [34]. And the UV–vis spectra of **1** in buffered aqueous solutions in pH 5.2 to 11.2 exhibit similar peaks to those in water. When pH = 12.0, the absorption band at 234 nm disappeared, suggesting that complex **1** decomposes to a new component under these conditions (Fig. S2). Therefore, we will explore its electrochemical properties in pH 5.2 to 11.2.

3.2. Cyclic voltammetry studies

The cyclic voltammogram (CV) of an aqueous solution of **1** (Fig. 1) shows a quasi-reversible wave at $E_{1/2}$ = −0.35 V (all potentials *vs* Ag/AgCl), which can be assigned to $Cu^{II}Cu^{II}/Cu^{II}Cu^{I}$ couple. Sweeping toward the anode shows two irreversible wave at 0.87 and 1.25 V, which are assigned to $Cu^{III}Cu^{II}/Cu^{II}Cu^{II}$ and $Cu^{III}Cu^{III}/Cu^{III}Cu^{II}$ couples, respectively.

We further explored the electrochemical behavior of **1** in buffered aqueous solution where pH = 5.7–11.2 which is the range associated with catalytic water reduction and oxidation. In pH 7.0 phosphate buffer, the reversible $Cu^{II}Cu^{II}/Cu^{II}Cu^{I}$ wave at −0.35 V was also observed for **1** (Fig. S3). The $Cu^{II}Cu^{II}/Cu^{II}Cu^{I}$ couple displays a pH-dependent redox potential change, with a slope of −55 mV pH^{-1} in the range from pH 7.9 to 10.1 (Fig. 2), suggesting a proton-coupled electron transfer process. CVs were also recorded at different scan rates in order to obtain kinetic information of this complex. The current response of the redox event at about −0.35 V shows a linear dependence on the square root of the scan rate (Fig. S4), which is an indicative of a diffusion-controlled process, with the electrochemically active species freely diffusing in the solution. Correspondingly, sweeping toward the cathode reveals two irreversible redox waves at about −0.51 and −1.10 V, which are assigned to $Cu^{II}Cu^{I}/Cu^{I}Cu^{I}$ and $Cu^{I}Cu^{I}/Cu^{I}Cu^{0}$ couples, respectively (Fig. S3). The current response of the redox events at −1.10 V also

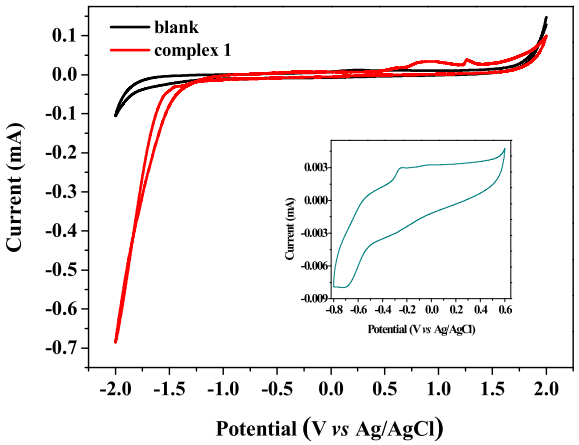

Fig. 1. Cyclic voltammograms of 0.10 M KNO_3 aqueous solution without and with 1.196 mM complex **1** at a glassy carbon electrode and a scan rate of 100 mV s^{-1}. The inset shows a magnified view of the $Cu^{II}Cu^{II}/Cu^{II}Cu^{I}$ couple.

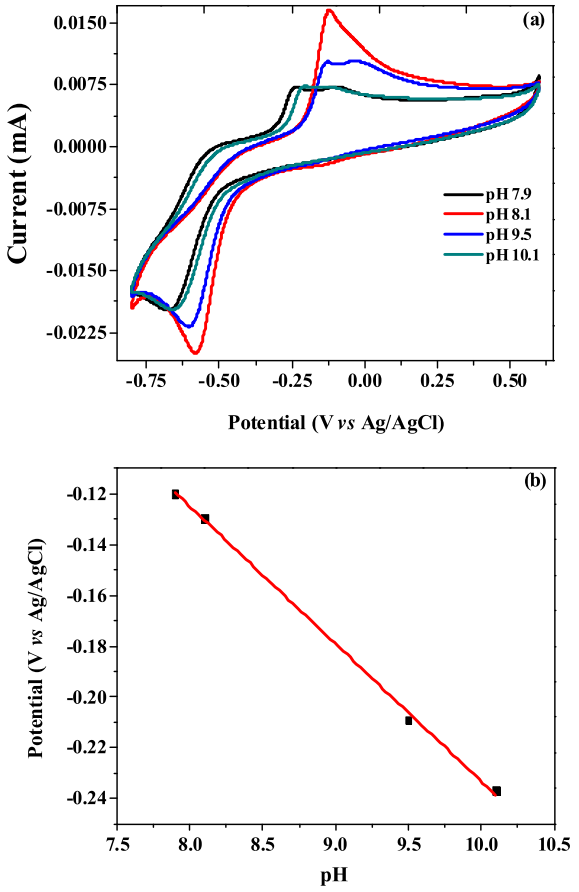

Fig. 2. (a) Cyclic voltammograms of complex **1** (1.196 mM) in different pHs. Conditions: 0.25 M phosphate buffer, scan rate = 100 mV s^{-1}, GC working electrode (1 mm diameter), Pt wire counter electrode, Ag/AgCl reference electrode. (b) Pourbaix diagram for the $Cu^{II}Cu^{II}/Cu^{II}Cu^{I}$ couple of complex **1**.

varies linearly on the square root of the scan rate (pH 7.0), which is an indicative of a diffusion-controlled process (Fig. S5). Sweeping toward the anode shows one irreversible redox wave at about 1.08 V (pH 7.0), which can be assigned to a metal-based $Cu^{III}Cu^{II}/Cu^{II}Cu^{II}$ process (Fig. S3).

A number of control experiments were carried out to verify that complex **1** is responsible for the catalysis. In particular, the free ligand, $CuSO_4$, and a mixture of the free ligand and $CuSO_4$ were each measured under identical conditions. As can be seen in Figs. S6–Fig. S8, the catalytic competency achieved with **1** is not matched by either the free ligand alone, $CuSO_4$, or the mixture of the free ligand and $CuSO_4$, as might arise from dissociation of the ligand; nor can it be accomplished with the ligand bound to a redox-inactive metal. Thus, a combination of the redox-active copper and the ligand is essential for catalytic activity.

3.3. Catalytic hydrogen evolution in water

First, we explored the catalytic water reduction by complex **1**. As shown in Fig. 3(a), **1** shows a pH-dependent peak between −1.25 and −1.75 V versus Ag/AgCl. Cyclic voltammogram of background in the absence of complex **1** exhibits no catalytic current at the potential of the couples of $Cu^{II}Cu^{I}/Cu^{I}Cu^{I}$ and $Cu^{I}Cu^{I}/Cu^{I}Cu^{0}$ (Fig. S3), suggesting that water reduction to H_2 occurs with complex **1** [17]. On the basis of literature precedent [35] and above analyses, we propose the catalytic cycle depicted in Scheme 1 for the generation of hydrogen from water mediated by **1**. Two-

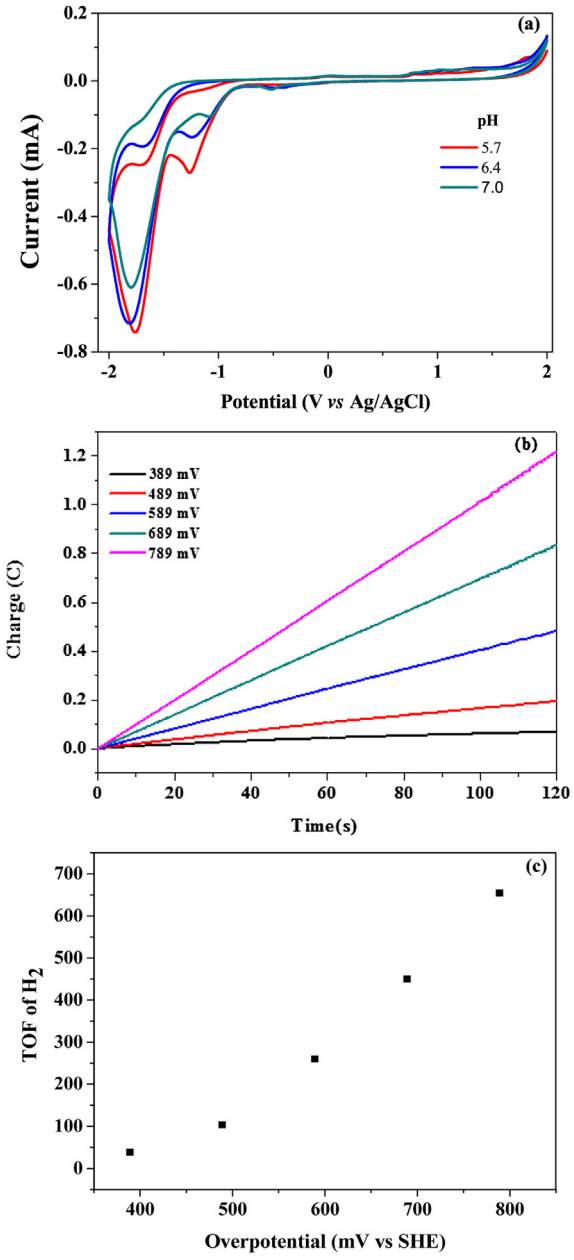

Fig. 3. (a) Cyclic voltammograms of complex **1** (1.196 mM) in 0.25 M buffer (pH 3.6, 4.8, 5.6, 6.0, 6.5, 7.0) at a glassy carbon electrode and a scan rate of 100 mV s^{-1} for water reduction. (b) Charge buildup of complex **1** (1.196 mM) versus overpotentials (mV versus SHE) at pH 7.0. All data have been deducted blank. (c) Turnover frequency (mol H_2/mol catalysts/h) for electrocatalystic hydrogen production by complex **1** (1.196 mM) under overpotentials (mV versus SHE).

electron reduction of $[Cu^{II}(Me_2oxpn)Cu^{II}(OH)_2]$ gives a putative $[Cu^{I}(Me_2oxpn)Cu^{I}(OH)_2]^{2-}$ species (A). Addition of water yields the Cu^{III}-H species (B), a high reactive intermediate. Further reduction of the Cu^{III}-H species affords H_2, releases two OH^- anions and regenerates the starting complex **1**. Further mechanistic studies are under investigation, because this is the first time that a copper(II) complex is used to catalyze hydrogen evolution from purely aqueous solution.

Fig. 3(b) shows the total charge of bulk electrolysis of complex **1** at pH 7.0. When the applied potential was −1.45 V *vs* Ag/AgCl, the maximum charge was only 128 mC during 2 min of electrolysis in absence of complex **1** (Fig. S9). Under the same conditions, the

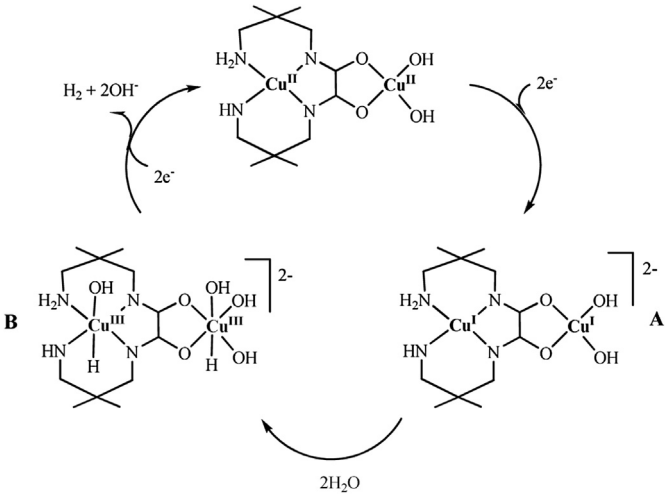

Scheme 1. The possible catalytic mechanism for water reduction by complex **1**.

charge reached 1590 mC with addition of complex **1**, with accompanying evolution of a gas, which was confirmed as H_2 by gas chromatography. According to Fig. 4(a), ~19.5 mL of H_2 was produced over an electrolysis period of 1 h with a Faradaic efficiency of 95% for H_2 (Fig. 4(b)). TOF for electrocatalytic hydrogen production by complex **1** is 654 (pH 7.0) moles of hydrogen per mole of catalyst per hour at an overpotential of 789 mV *vs* SHE (Fig. 3(c)). To the best of our knowledge, this value is significantly higher than some reported molecular catalysts for electrochemical hydrogen production from neutral water, including a dinickel complex that exhibits a turnover number of 100 mol of H_2 per mole of catalyst with a turnover frequency of 160 mol of H_2 per mole of catalyst per hour at an overpotential of 820 mV [36] and a cobalt complex displaying a turnover number of 5 mol of H_2 per mole of catalyst with a turnover number of 0.4 mol of H_2 per mole of catalyst per hour at an overpotential of 390 mV [37], and are comparable to a molybdenum-oxo complex that shows a maximum of 1600 mol of H_2 per mole of catalyst per hour at an overpotential of 642 mV [17].

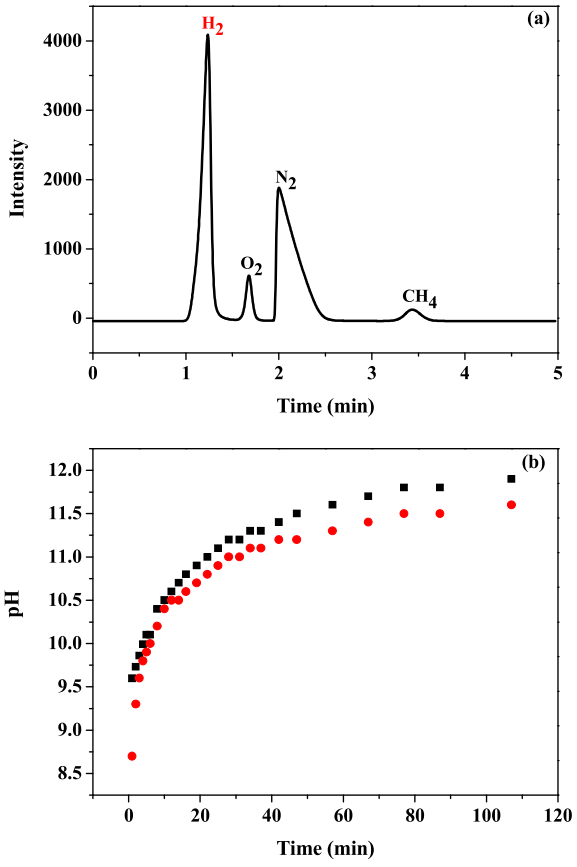

Fig. 4. (a) GC traces after a 1-h controlled-potential electrolysis at −1.20 V *vs* SHE of 5.74 μM complex **1** in 0.25 M phosphate buffer, pH 7.0. A standard of CH_4 was added for calibration purposes. (b) Measured (black) and calculated (red) pH changes assuming a 100% Faradic efficiency of complex **1** during electrolysis. (The theoretical pH change over time can be calculated by the equation of $pH = 14 + \lg \frac{\sum It}{FV}$ where I = current (A), t = time (s), F = Faraday constant (96,485 C mol^{-1}), V = solution volume (0.05 L)).(For interpretation of the references to colour in this figure legend, the reader is referred to the web version of this article.)

3.4. Catalytic water oxidation

To explore the catalytic water oxidation by complex **1**, CVs were conducted in buffer at different pH values. At more positive potentials, two irreversible oxidation waves appeared at 0.90 and 1.26 V *vs* Ag/AgCl in 0.25 M buffer, corresponding to $Cu^{III}Cu^{II}/Cu^{II}Cu^{II}$ and $Cu^{III}Cu^{III}/Cu^{III}Cu^{II}$ couples, respectively (Fig. S3). Fig. 5(a) exhibits a systematic increase in i_{cat} with increasing pH from 7.0 to 11.2. Cyclic voltammograms of background in the absence of complex **1** exhibit no catalytic current at the potential of the couple of $Cu^{III}Cu^{II}/Cu^{II}Cu^{II}$, suggesting that water oxidation to O_2 occurs with complex **1** [38]. The current enhancements for waves at about

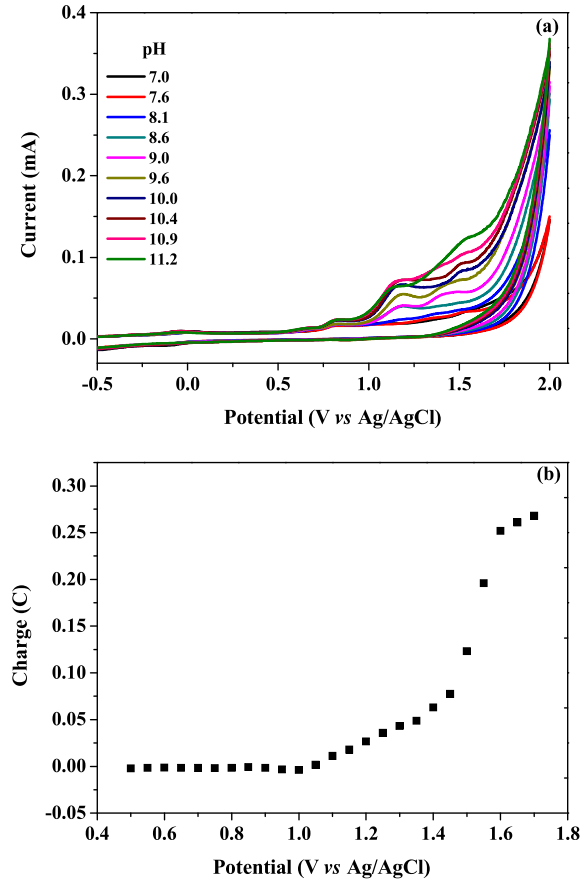

Fig. 5. (a) Cyclic voltammograms of complex **1** (5.74 μM) in 0.25 M buffer (pH 7.0–11.2). (b) Charge buildup of complex **1** (5.74 μM) versus applied potentials (pH 10.4). Conditions: Pt counter electrode, Ag/AgCl reference electrode, scan rate 100 mV s^{-1},2 min. All data have been deducted blank.

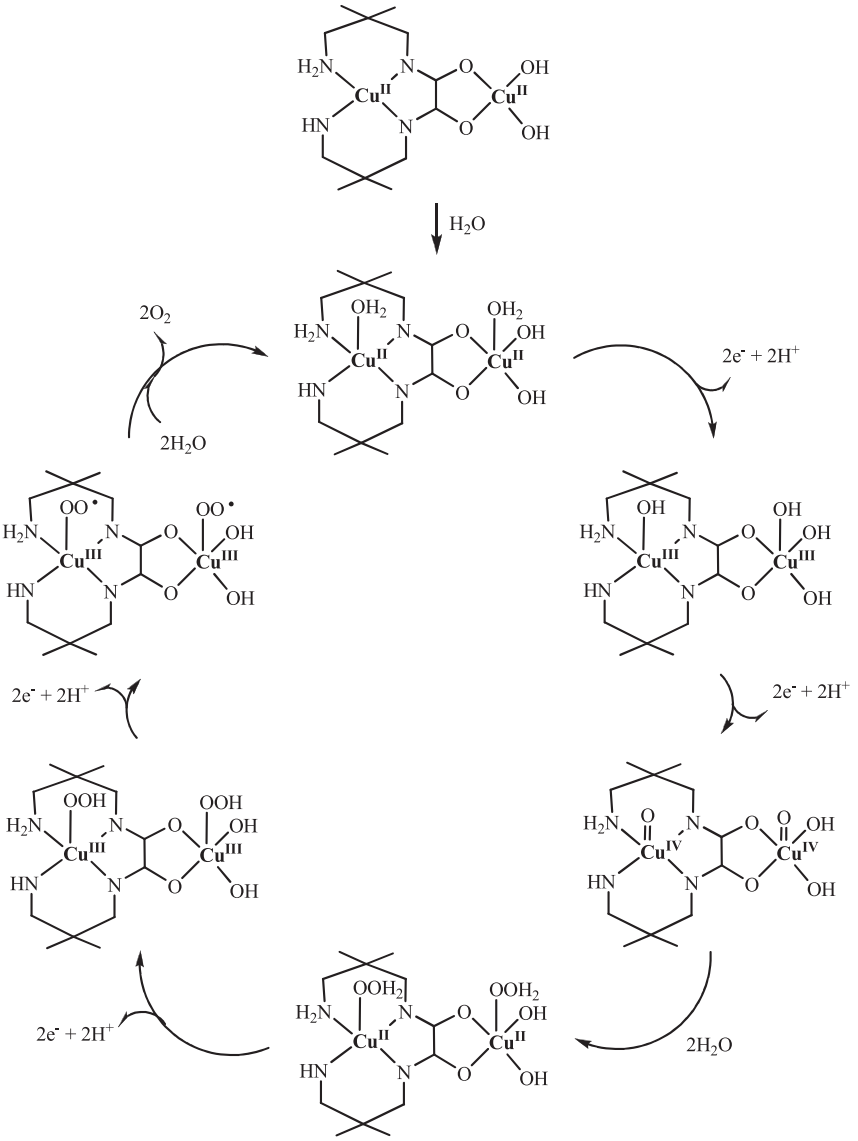

Scheme 2. The possible catalytic mechanism for water oxidation by complex **1**.

$E_{p,a}$ = 1.12 and 1.45 V are consistent with catalytic water oxidation, with catalytic onset shift to more negative potentials (from 1.70 V to 0.80 V).

Within the pH range 7.0–8.1, only one redox wave at about 0.80 V ($Cu^{III}Cu^{II}/Cu^{II}Cu^{II}$) was observed. When the pH was 8.6, CV of complex **1** exhibited one new redox wave at about 1.12 V, which is assigned to the $Cu^{III}Cu^{III}/Cu^{III}Cu^{II}$ couple. When the pH was 9.0, CV of complex **1** showed another new peak at about 1.45 V, which can be assigned to the couple $Cu^{IV}Cu^{III}/Cu^{III}Cu^{III}$ and indicating a new component was formed. When the pH reached 10.9, the irreversible oxidation wave at about 1.45 V got decay, indicating complex **1** was decomposing. The current enhancement for the wave at about $E_{p,a}$ = 0.86 V ($Cu^{III}Cu^{II}/Cu^{II}Cu^{II}$) is consistent with catalytic water oxidation in pH 7.0–11.2, with catalytic onset shift to more negative potentials (from 1.70 V to 0.68 V). For the wave at about $E_{p,a}$ = 1.12 V ($Cu^{III}Cu^{III}/Cu^{III}Cu^{II}$), catalytic water oxidation occurs at pH 8.6 to 11.2, with catalytic onset shift to more negative potentials (from 1.70 V to 0.95 V). And catalytic water oxidation by $Cu^{IV}Cu^{III}/Cu^{III}Cu^{III}$ ($E_{p,a}$ = 1.45 V) occurs at pH 8.6 to 10.9, with catalytic onset shift to more negative potentials (from 1.70 V to 1.32 V). Based on the above observations, all three couples of $Cu^{III}Cu^{II}/Cu^{II}Cu^{II}$, $Cu^{III}Cu^{III}/Cu^{III}Cu^{II}$ and $Cu^{IV}Cu^{III}/Cu^{III}Cu^{III}$ are devoted to water oxidation, but the $Cu^{III}Cu^{II}/Cu^{II}Cu^{II}$ couple plays a relatively small role. Based on these observations, a mechanism for water oxidation is proposed in Scheme 2. In this mechanism, the product of the second oxidation would be the formally $Cu^{IV}Cu^{IV}$ species, a high-oxidation Cu-oxo intermediate as sites for O–O coupling and water oxidation, as found in other complexes [39–42].

Analysis of the anodic scans of the redox couples at 1.12 and 1.45 V as a function of scan rates (Fig. S10) both show a linear relation, consistent with adsorption of the molecules on the electrode surface. Such distinctive electrochemical properties suggest the possible usage of this complex as an electrocatalyst for hydrogen evolution reaction.

Further evidence for water oxidation by complex **1** was obtained by bulk electrolysis of an aqueous solution of complex **1** (5.74 μM) with phosphate buffer (0.25 M) at variable potential using an ITO electrode in a double-compartment cell. A series of applied potentials were chosen, corresponding to the electro-catalytic potentials observed in cyclic voltammograms. As shown in Fig. 5(b) (pH 10.4), the amount of charge used in 2 min increases with increasing the applied potential, accompanying the formation of a

large amount of gas bubble, can be attributed to the catalytic generation of O_2 from water.

For the redox $Cu^{III}Cu^{III}/Cu^{III}Cu^{II}$ couple, water oxidation occurs at an overpotential of 460 mV *vs* SHE, based on the half-peak potential for CVs at pH 10.4 and 100 mV s^{-1}, and the reversible potential for $4e^- + O_2 + 4H^+ = 2H_2O$ of 0.613 V at this pH. This overpotential is the lowest among the reported homogeneous water oxidation catalysts (600–900 mV) [19,21,26,43–46]. Compared to the $Cu^{III}Cu^{III}/Cu^{III}Cu^{II}$ couple, water oxidation by $Cu^{IV}Cu^{III}/Cu^{III}Cu^{III}$ occurs at an overpotential of 935 mV *vs* SHE, based on the half-peak potential for CVs at pH 10.4 and 100 mV s^{-1}, and the reversible potential for $4e^- + O_2 + 4H^+ = 2H_2O$ of 0.613 V at this pH.

Evolution of O_2 as a product was investigated by controlled-potential electrolysis at 1.23 V *vs* Ag/AgCl on a large surface area ITO (1.32 cm^2) electrode with 2.8 μM complex **1** in 0.25 M phosphate buffer (pH 10.4). The background for oxygen formation at the applied potential in the absence of catalyst is small (Fig. S11). After a 5 h electrolysis period, pH decreased by 2.0 units (from 9.5 to 7.5), consistent with consumption of OH^- by water oxidation, $4OH^- + 4e^- \rightarrow 2O_2 + 2H_2O$. The evolved O_2 was analyzed by gas chromatography, Fig. 6(a), which gave ~38.8 μmol of O_2 over an electrolysis period of 5 h with a Faradaic efficiency of 90% for O_2 (Fig. 6(b)).

This study stated clearly that **1** is capable of catalyzing the oxidation of water to O_2. According to Eq. (1) [25], n_p is the number of electrons transferred in the noncatalytic wave, n_c is the moles of electrons required to generate a mol of O_2 and ν is the scan rate. From the slope of the plot of i_{cat}/i_d versus $\nu^{-1/2}$ (Fig. 7), we calculated k_{cat}, which is usually referred as turnover frequency (TOF) of the catalyst in the literature, for the catalyst reaching a maximum of 2.14 s^{-1} ($E_{p,a}$ = 1.12 V, and Eq. (2)), and 2.56 s^{-1} ($E_{p,a}$ = 1.45 V, and Eq. (3)), respectively, indicating that both $Cu^{III}Cu^{III}/Cu^{III}Cu^{II}$ and $Cu^{IV}Cu^{III}/Cu^{III}Cu^{III}$ are devoted to water oxidation. These values are higher than some reported molecular water oxidation catalysts [26,42,47], yet lower than the recently reported copper-based ones [24,39].

$$\frac{i_c}{i_p} = 0.359\frac{n_c}{n_p^{3/2}}\sqrt{k_{cat}/\upsilon} \quad (1)$$

The durability of catalyst **1** for water reduction and oxidation were also tested in an extended CPE experiment performed in a 0.25 M buffer at pH 7.0 and pH 10.4, respectively. As depicted in Fig. S12, the catalyst affords a robust and essentially linear charge build-up over time, with no substantial loss in activity over the course of 32 h for water reduction. After a 32 h electrolysis period, the charge build-up slightly increased due the increase in pH, consistent with accumulation of OH^- by water reduction, $2H_2O + 2e^- \rightarrow H_2 + 2OH^-$, suggesting that catalyst **1** decomposes to an inactive species at high pH. The original catalytic function was recovered and can be repeated at least 10 times when the solution pH was adjusted back to the original 7.0. And the catalyst also affords a robust charge build-up over time, with no substantial loss in activity over the course of 72 h for water oxidation (Fig. S13).

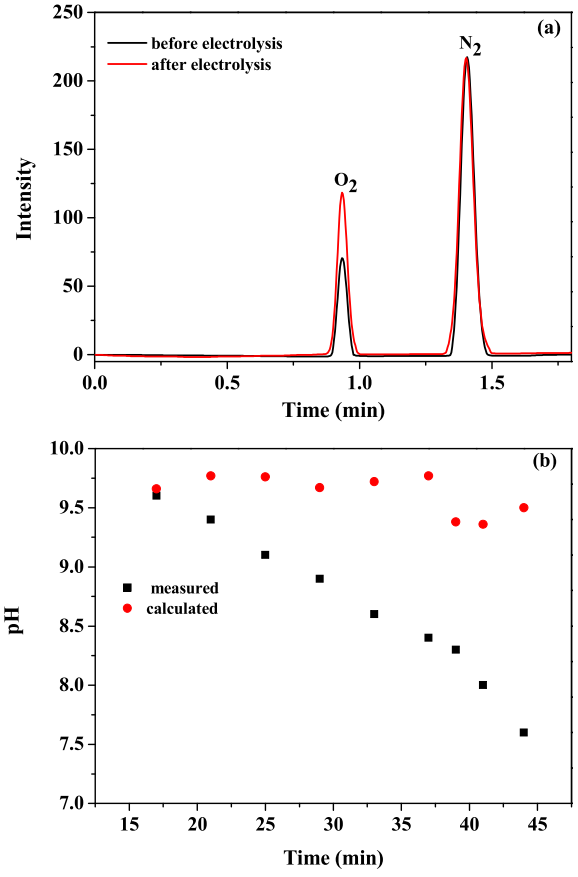

Fig. 6. (a) Normalized gas chromatographic trace before (black line) and after (red line) electrolysis in the presence of 2.8 μM complex **1** for 5 h. 0.25 M phosphate buffer, pH 10.4, ITO working electrode (1.32 cm^2), Pt counter electrode, Ag/AgCl reference electrode, applied potential 1.20 V *vs* Ag/AgCl. (b) Measured (black) and calculated (red) pH changes assuming a 100% Faradaic efficiency of complex **1** during the electrolysis. (For interpretation of the references to colour in this figure legend, the reader is referred to the web version of this article.)

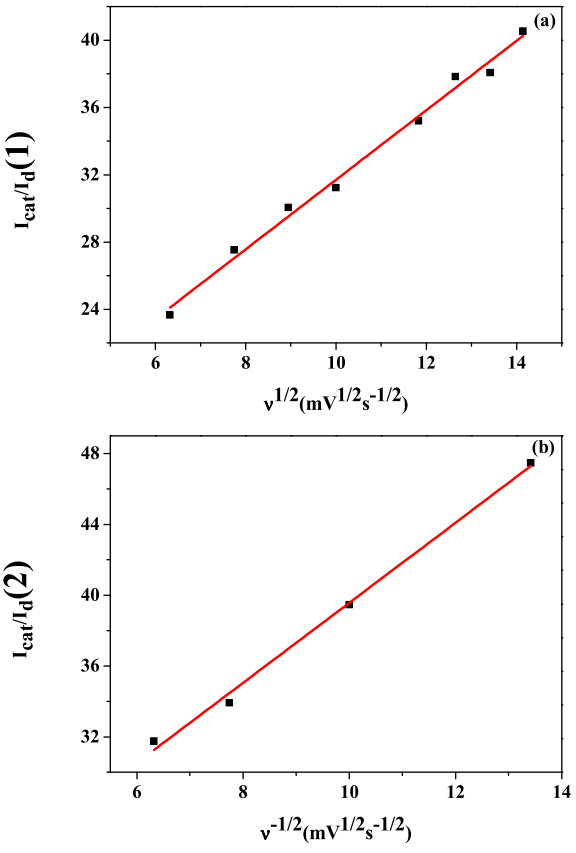

Fig. 7. Linear fitting plot of i_{cat}/i_d *vs* $\nu^{-1/2}$ for the couples $Cu^{III}Cu^{III}/Cu^{III}Cu^{II}$ (a) and $Cu^{VI}Cu^{III}/Cu^{III}Cu^{III}$ (b).

To prove complex **1** as a homogeneous electrocatalyst, we obtained dependence of the catalytic current on complex **1** concentration. As shown in Fig. S14, the observation of the catalytic current being dependent of the complex concentration could indicate a homogeneous catalyst. And several pieces of evidence also suggest that this copper complex is a homogeneous catalyst: 1) There is no evidence for a heterogeneous electrocatalytic deposit. For example, the electrode was rinsed with water and electrolysis at −1.45 V *vs* Ag/AgCl was run for an additional 2 min in a 0.25 M phosphate buffer at pH 7.0 with no catalyst present in solution. During this period, ca. 128 mC of charge was passed, a similar magnitude as is observed for electrolysis conducted with freshly polished electrodes. 2) No discoloration of the electrodes was observed during cyclic voltammetry or bulk electrolysis. 3) Under the same conditions, at a GC electrode, there was no evidence for precipitation formation by ICP (Fig. S15) after a 2 h electrolysis period.

4. Conclusions

In summary, a water soluble dinuclear copper complex $Cu(Me_2oxpn)Cu(OH)_2$] **1**, which is very easy to be obtained, can catalyze both water oxidation and reduction. Electrochemical studies show that **1** is a soluble molecular copper species, that is among the most rapid homogeneous water reduction catalysts, with a TOF of 654 (pH 7.0) moles of hydrogen per mole of catalyst per hour at an overpotential of 789 mV *vs* SHE. Water oxidation occurs at an overpotential of 636 mV *vs* SHE to give O_2 with a turnover frequency (TOF) of ~2.14 s^{-1} (pH 10.4). This discovery has established a new chemical paradigm for creating water oxidation and reduction catalysts that is highly active and robust in purely aqueous media. Our ongoing efforts are focused on modifying the ligands to give related water soluble complexes for further functional studies, with an emphasis on chemistry relevant to sustainable energy cycles.

Acknowledgments

This work was supported by 1) the National Science Foundation of China (No. 20971045, 21271073), and 2) the Student Research Program (SRP) of South China University of Technology (No. B15-B7050170).

Appendix A. Supplementary data

Supplementary data related to this article can be found at http://dx.doi.org/10.1016/j.jpowsour.2014.09.075.

References

[1] W.J. Youngblood, S.A. Lee, Y. Kobayashi, E. Hernandez-Pagan, P.G. Hoertz, T.A. Moore, A.L. Moore, D. Gust, T.E. Mallouk, J. Am. Chem. Soc. 131 (2009) 926–927.
[2] S.Y. Reece, J.A. Hamel, K. Sung, T.D. Jarvi, A.J. Esswein, J.J.H. Pijpers, D.G. Nocera, Science 334 (2011) 645–648.
[3] T. Ohno, L. Bai, T. Hisatomi, K. Maeda, K. Domen, J. Am. Chem. Soc. 134 (2012) 8254–8259.
[4] Y. Gao, X. Ding, J. Liu, L. Wang, Z. Lu, L. Li, L. Sun, J. Am, Chem. Soc. 135 (2013) 4219–4222.
[5] J.R. Swierk, T.E. Mallouk, Chem. Soc. Rev. 42 (2013) 2357–2387.
[6] B.J. Fisher, R. Eisenberg, J. Am. Chem. Soc. 102 (1980) 7361–7363.
[7] M.L. Helm, M.P. Stewart, R.M. Bullock, M.R. DuBois, D.L. DuBois, Science 333 (2011) 863–866.
[8] W.A. Hoffert, J.A.S. Roberts, R.M. Bullock, M.L. Helm, Chem. Commun. 49 (2013) 7767–7769.
[9] J.P. Cao, T. Fang, L.Z. Fu, L.L. Zhou, S.Z. Zhan, Int. J. Hydrogen Energy 39 (2014) 10980–10986.
[10] M.A. Gross, A. Reynal, J.R. Durrant, E. Reisner, J. Am. Chem. Soc. 136 (2014) 356–366.
[11] J.G. Kleingardner, B. Kandemir, K.L. Bren, J. Am. Chem. Soc. 136 (2014) 4–7.
[12] W.M. Singh, T. Baine, S. Kudo, S. Tian, X.A.N. Ma, H. Zhou, Angew. Chem. Int. Ed. 51 (2012) 5941–5944.
[13] Y. Sun, J.P. Bigi, N.A. Piro, M.L. Tang, J.R. Long, C.J. Chang, J. Am. Chem. Soc. 133 (2011) 9212–9215.
[14] B.D. Stubbert, J.C. Peters, H.B. Gray, J. Am. Chem. Soc. 133 (2011) 18070–18073.
[15] L. Tong, R. Zong, R.P. Thummel, J. Am. Chem. Soc. 136 (2014) 4881–4884.
[16] H.S. Ahn, T.C. Davenportab, T.D. Tilley, Chem. Commun. 50 (2014) 3834–3837.
[17] H.I. Karunadasa, C.J. Chang, J.R. Long, Nature 464 (2010) 1329–1333.
[18] (a) V.S. Thoi, H.I. Karunadasa, Y. Surendranath, J.R. Long, C.J. Chang, Energy Environ. Sci. 5 (2012) 7762–7770;
(b) J. Limburg, J.S. Vrettos, L.M. Liable-Sands, A.L. Rheinglod, R.H. Crabtree, G.H. Brudvig, Science 283 (1999) 1524–1527.
[19] G.C. Dismukes, R. Brimblecombe, G.A.N. Felton, R.S. Prydun, J.E. Sheats, L. Spiccia, G.F. Swiegers, Acc. Chem. Res. 42 (2009) 1935–1943.
[20] Y. Gao, R.H. Crabtree, G.W. Brudvig, Inorg. Chem. 51 (2012) 4043–4050.
[21] Q. Yin, J.M. Tan, C. Besson, Y.V. Geletii, D.G. Musaev, A.E. Kuznetsov, Z. Luo, K.I. Hardcastle, C.L. Hill, Science 328 (2010) 342–345.
[22] D.K. Dogutan, R. McGuire, D.G. Nocera, J. Am. Chem. Soc. 133 (2011) 9178–9180.
[23] D.J. Wasylenko, C. Ganesamoorthy, J. Borau-Garcia, C.P. Berlinguette, Chem. Commun. 47 (2011) 4249–4251.
[24] S.M. Barnett, K.I. Goldberg, J.M. Mayer, Nat. Chem. 4 (2012) 498–502.
[25] T. Zhang, C. Wang, S. Liu, J. Wang, W. Lin, J. Am. Chem. Soc. 136 (2014) 273–281.
[26] W.C. Ellis, N.D. McDaniel, S. Bernhard, T.J. Collins, J. Am. Chem. Soc. 132 (2010) 10990–10991.
[27] J. Lloret-Fillol, Z. Codol, I. Garcia-Bosch, L. Gmez, J.J. Pla, M. Costas, Nat. Chem. 3 (2011) 807–813.
[28] R. Sarma, A.M. Angeles-Boza, D.W. Brinkley, J.P. Roth, J. Am. Chem. Soc. 134 (2012) 15371–15386.
[29] D. Hong, Y. Yamada, T. Nagatomi, Y. Takai, S. Fukuzumi, J. Am. Chem. Soc. 134 (2012) 19572–19575.
[30] G. Chen, L. Chen, S. Ng, W. Man, T. Lau, Angew. Chem. Int. Ed. 52 (2013) 1789–1791.
[31] M.K. Coggins, M. Zhang, A.K. Vannucci, C.J. Dares, T.J. Meyer, J. Am. Chem. Soc. 136 (2014) 5531–5534.
[32] J. Ribas, A. Garcia, M. Monfort, Polyhedron 10 (1991) 103–106.
[33] Y. Journaux, J. Sletten, O. Kahn, Inorg. Chem. 24 (1985) 4063–4069.
[34] T.N. Sorrell, Tetrahedron 45 (1989) 3–68.
[35] S. Mandal, S. Shikano, Y. Yamada, Y.-M. Lee, W. Nam, A. Llobet, S. Fukuzumi, J. Am. Chem. Soc. 135 (2013) 15294–15297.
[36] J.P. Collin, A. Jouaiti, J.P. Sauvage, Inorg. Chem. 27 (1988) 1986–1990.
[37] P.V. Bernhardt, L.A. Jones, Inorg. Chem. 38 (1999) 5086–5090.
[38] P. Kang, E. Bobyr, J. Dustman, K.O. Hodgson, B. Hedman, E.I. Solomon, T.D.P. Stack, Inorg. Chem. 49 (2010) 11030–11038.
[39] M.-T. Zhang, Z. Chen, P. Kang, T.J. Meyer, J. Am. Chem. Soc. 135 (2013) 2048–2051.
[40] Z.F. Chen, J.J. Concepcion, X.Q. Hu, W.T. Yang, P.G. Hoertz, T.J. Meyer, Proc. Natl. Acad. Sci. U. S. A. 107 (2010) 7225–7229.
[41] D.J. Wasylenko, C. Ganesamoorthy, M.A. Henderson, B.D. Koivisto, H.D. Osthoff, C.P. Berlinguette, J. Am. Chem. Soc. 132 (2010) 16094–16106.
[42] J.F. Hull, D. Balcells, J.D. Blakemore, C.D. Incarvito, O. Eisenstein, G.W. Brudvig, R.H. Crabtree, J. Am. Chem. Soc. 131 (2009) 8730–8731.
[43] Y. Gorlin, T.F. Jaramillo, J. Am. Chem. Soc. 132 (2010) 13612–13614.
[44] R. Lalrempuia, N.D. McDaniel, H. Muller-Bunz, S. Bernhard, M. Albrecht, Angew. Chem. Int. Ed. 49 (2010) 9765–9768.
[45] N.D. Schley, J.D. Blakemore, N.K. Subbaiyan, C.D. Incarvito, F. D'Souza, R.H. Crabtree, G.W. Brudvig, J. Am. Chem. Soc. 133 (2011) 10473–10481.
[46] J.G. McAlpin, T.A. Stich, C.A. Ohlin, Y. Surendranath, D.G. Nocera, W.H. Casey, R.D. Britt, J. Am. Chem. Soc. 133 (2011) 15444–15452.
[47] J. Concepcion, J. Jurss, P. Hoertz, T. Meyer, Angew. Chem. Int. Ed. 48 (2009) 9473–9476.